NeuroImage 53 (2010) 506–514

Contents lists available at ScienceDirect

NeuroImage

journal homepage: www.elsevier.com/locate/ynimg

Differential effect of age on hippocampal subfields assessed using a new high-resolution 3T MR sequence

Renaud La Joie, Marine Fouquet, Florence Mézenge, Brigitte Landeau, Nicolas Villain, Katell Mevel, Alice Pélerin, Francis Eustache, Béatrice Desgranges, Gaël Chételat *

Inserm-EPHE, Université de Caen/Basse-Normandie, Unité U923, GIP Cyceron, CHU Côte de Nacre, Caen, France

ARTICLE INFO

Article history:
Received 17 March 2010
Revised 7 June 2010
Accepted 9 June 2010
Available online 16 June 2010

Keywords:
High-resolution MRI
Hippocampal subfields
Aging
CA1
Subiculum
VBM
Developmental hypothesis

ABSTRACT

Recent advances in neuroimaging have highlighted the interest to differentiate hippocampal subfields for cognitive neurosciences and more notably in assessing the effects of normal and pathological aging. The main goal of the present study is to investigate the effects of normal aging onto the volume of the different hippocampal subfields. For this purpose, we developed a new magnetic resonance sequence together with reliable tracing guidelines to assess the volume of different subfields of the hippocampus using a 3 Tesla scanner, and estimated the validity of a simpler and less time-consuming method based on the widely-used automatic Voxel-Based Morphometry (VBM) technique. Three hippocampal regions of interest were delineated on the right and left hippocampi of 50 healthy subjects between 18 and 68 years old corresponding to the CA1, subiculum and other (including CA2-3-4 and Dentate Gyrus) subfields. A strong effect of age was found on the volume of the subiculum only, with a decrease paralleling that of the global gray matter volume, while CA1 and other subfields seemed relatively spared. Although less precise than the ROI-tracing technique, the VBM-based method appeared as a reliable alternative especially to distinguish CA1 and subiculum subfields. Our findings of a specific effect of age on the subiculum are consistent with the developmental hypothesis ("last-in first-out" theory). This contrasts with the predominant vulnerability of the CA1 subfield to Alzheimer's disease reported in several previous studies, suggesting that the assessment of hippocampal subfields may improve the discrimination between normal and pathological aging.

Introduction

The hippocampus has been the focus of extensive research over the last decades, especially with the development and improvement of neuroimaging techniques. The particular interest of neuroscientists for this structure arises from its implication in cognitive processes, especially episodic memory (Lepage et al., 1998; Squire et al., 1992; Tulving and Markowitsch, 1998; see Spaniol et al., 2009 for review) and spatial navigation (Burgess et al., 2002; Ekstrom et al., 2003; Maguire et al., 1998; see Bird and Burgess, 2008 for review), as well as its structural alteration in several neurological and psychiatric disorders, such as Alzheimer's disease (AD), temporal lobe epilepsy, schizophrenia, post-traumatic stress disorder or major depression (see Geuze et al., 2005 for review). In AD, hippocampal atrophy is a consensual finding and an early process detectable years before the clinical diagnosis of AD using Magnetic Resonance Imaging (MRI) (Jack et al., 1992; Seab et al., 1988; see Chételat and Baron, 2003 for review). In contrast, hippocampal volume change over normal aging (NA) is still a source of debate as some studies showed it is preserved (Sullivan et al., 2005) or relatively preserved compared to the volume of the whole gray matter (Good et al., 2001; Grieve et al., 2005) while others pointed to its reduction with age (Lemaitre et al., 2005; Raz et al., 2004). Some of those discrepancies might be due to differences in the studied populations: (absolute or relative) preservation of the hippocampal volume was mostly found when the studied sample covered the whole adulthood (Good et al., 2001; Kalpouzos et al., 2009; Sullivan et al., 2005) while studies showing a significant decline with age only assessed elder subjects (Lemaitre et al., 2005; Jack et al., 1997), suggesting that this change only occurs in late adulthood. This hypothesis of a non-linear relationship between age and hippocampal volume is now supported by several longitudinal studies showing an increasing rate of hippocampal shrinkage with age (Fjell et al., 2009; Raz et al., 2004).

Yet, the issue of the evolution of the anatomy of the hippocampus needs to be more specifically addressed, not only to further improve our understanding on normal aging processes, but also to refine the delineation of the boundary between normal and pathological processes and thus to improve the early identification of AD cases.

The hippocampus is composed of several histologically defined and interconnected subfields, including the Dentate Gyrus (DG), the four fields of the Cornu Ammonis (CA1–4) and the subiculum (Duvernoy, 1998). Recent advances in neuroimaging stress the relevance to take into account these different sub-structures instead of assessing the hippocampus as a

* Corresponding author. Laboratoire de Neuropsychologie, Inserm-EPHE, Université de Caen/Basse-Normandie, Unité U923, GIP Cyceron, Bd H Becquerel, 14074 Caen cedex, France.
E-mail address: chetelat@cyceron.fr (G. Chételat).

1053-8119/$ – see front matter © 2010 Elsevier Inc. All rights reserved.
doi:10.1016/j.neuroimage.2010.06.024

whole. For instance, studies using high-resolution functional MRI showed a distinct involvement of the different hippocampal subfields in encoding versus retrieval memory processes (Eldridge et al., 2005; Zeineh et al., 2003) and a specific role for CA1 in the encoding of allocentric information (Suthana et al., 2009). Importantly, it seems that hippocampal subfields are also differentially vulnerable to neurological disorders and particularly AD, with the CA1 showing highest and earliest sensitivity in both neuropathological (West et al., 1994) and imaging (Apostolova et al., 2008; Chételat et al., 2008; Csernansky et al., 2005; Frisoni et al., 2008; Wang et al., 2006) studies.

A few surface-based methods have been developed in the past few years to map age or AD-related changes in the shape of the hippocampus based on an estimation of surface changes, such as radial atrophy (Apostolova et al., 2006; Frisoni et al., 2008; Thompson et al., 2004) or large-deformation high-dimensional brain mapping (Csernansky et al., 2005; Wang et al., 2003). These approaches provide valuable information on hippocampal surface changes allowing localisation of hippocampal areas of highest inward and outward transformations without requiring individual delineation of each hippocampal subfield. On the other hand, they do not directly provide quantitative information on hippocampal subfields volumes allowing the estimation of volumetric changes associated to normal aging or brain disorders. Moreover, these surface approaches estimate changes in the external boundaries of the hippocampus only, so that they will not detect modifications that may occur within this structure such as an increase in the number or volume of intra-hippocampal cerebrospinal fluid (CSF) spaces (including residual cavities of the vestigial hippocampal sulcus as well as uncal sulcus). Importantly, such modifications may occur with age or pathology (Barboriak et al., 2000; Nakada et al., 2005; Yoneoka et al., 2002) although this point is quite controversial (Bastos-Leite et al., 2006; Li et al., 2006).

In a previous work (Chételat et al., 2008), we used a different method based on the widely used Voxel Based Morphometry (VBM) approach to map the effect of age, Mild Cognitive Impairment (MCI) and AD on the gray matter (GM) integrity of the hippocampus. Our findings were consistent with previous works using other methodologies, showing a predominant effect of age on the subiculum while the CA1 subfield was predominantly altered in MCI and AD. Yet, this particular technique still need to be validated against a reference state-of-the-art method, especially as the spatial normalization and smoothing steps of this technique may alter its sensitivity.

Recently developed high field MR sequences achieve a much better in-plane resolution than classic 1.5T MRI, allowing to assess the hippocampus *in vivo* at a submillimetric resolution on coronal slices at 3T (Eriksson et al., 2008; Nakada et al., 2005), 4T (Mueller et al., 2007; Mueller et al., 2008; Mueller and Weiner, 2009), 4.1T (Pan et al., 1995), 4.7T (De Vita et al., 2003; Malykhin et al., 2010) or 7T (Cho et al., 2010; Theysohn et al., 2009; Thomas et al., 2008). While automatic segmentation procedures of hippocampal subfields are being developed (Van Leemput et al., 2009), high-resolution MR images can be used to manually delineate hippocampal subfields using landmarks described in anatomic atlases (Malykhin et al., 2010; Mueller et al., 2007; Mueller et al., 2008; Mueller and Weiner, 2009). To date, the assessment of the effect of age on the volume of the hippocampal subfields obtained using manual delineation has only been performed in two previous studies, showing a significant effect of age on the volume of CA1 (Mueller et al., 2007), CA3 and DG (Mueller and Weiner, 2009). While these studies have offered a considerable contribution to the field, the method for manual delineation still needs to be improved. In these previous aging studies, manual tracings were only performed on 3 consecutive coronal slices centered on the body of the hippocampus, thus excluding most anterior and posterior parts of the hippocampus. This result in an under-estimation of hippocampal subfields volume and may reduce the sensitivity to detect specific changes, especially considering recent evidences of an antero-posterior gradient in the effect of age on the hippocampus volume with greatest reduction in its posterior part (Kalpouzos et al., 2009; Malykhin et al., 2008).

The present study was thus motivated by growing interests in the assessment of the different hippocampal subfields, notably to further understand the effect of age on hippocampal anatomy, stressing the need for a refined and very precise method to achieve this goal. The main objective of the present study was thus to assess the effects of age on the volumes of the different hippocampal subfields on a sample of 50 healthy subjects aged 19 to 68 years. For this purpose: (i) an MR sequence specifically designed to assess the hippocampus with a submillimetric resolution using a 3T scanner and a reasonable acquisition time (<10 min) to limit movement artefacts and facilitate clinical application is proposed; (ii) detailed guidelines for delineation of the hippocampal subfields covering most of its antero-posterior axis are provided; (iii) the reliability of these guidelines is assessed thanks to double delineation on a subsample of 15 healthy subjects; and (iv) the validity of a less precise but also less time-consuming automatic voxel-based approach to detect age effects on the hippocampal subfields is evaluated.

Methods

Participants

Healthy subjects were enrolled in this study after detailed clinical and neuropsychological examinations. Subjects were screened for the lack of abnormalities according to stringent inclusion/exclusion criteria including (1) normal somatic examination, (2) body mass index in the normal range, (3) no known vascular risk factor and smoking less than 10 cigarettes per day, (4) no alcohol or drug abuse, (5) blood pressure within normal limits (6) no history or clinical evidence of neurological disease, dementia or psychiatric disorder, (7) no current use of medication (except birth control pills, oestrogen replacement therapy and anti-hypertensive drugs), (8) normal standard T1- and T2-weighted MRI as assessed by a medical doctor. The Mattis dementia rating scale (Mattis, 1976) was used for subjects over 50 years old to exclude those with scores below the normal range for age. All subjects included in this study also underwent cognitive tasks assessing episodic memory, semantic memory and executive functions. They all had performances in the normal range (i.e. within 1.65 standard deviation of the normal mean for age, gender and education) in all cognitive tests, and no subject complained about his/her memory. This protocol was approved by the regional ethics committee and subjects gave written informed consent to the procedure prior to the investigation.

A total of fifty right-handed healthy subjects aged 19 to 68 years old (mean 39,9 ± 15,2) satisfying all selection criteria were included in the present study, including 31 women and 19 men who did not differ in age (women: 40.0 ± 14.7; men: 39.7 ± 16.3; Mann–Whitney $U = 286$; $p > 0.8$) or years of education (women: 13.4 ± 3.4; men: 13.2 ± 3.1; Mann–Whitney $U = 294{,}5$; $p > 0.9$). There were a trend for a decrease in years of education with age (Pearson's correlation $r = -0.278$; $p < 0.06$), so that years of education was corrected for in all statistical analyses. For the 15 subjects over 50, MMSE scores were 29.7 ± 0.59 [from 28 to 30] and Mattis score ranged from 138 to 144 (mean: 142.1 ± 1.9; maximal possible score = 144).

MRI data acquisition

Each subject underwent an MRI examination at the CYCERON center (Caen, France) using a 3T Philips (Eindhoven, The Netherlands) camera. First, T1-weighted structural images were acquired (Repetition Time (TR) = 20 ms; Echo Time (TE) = 4.6 ms; flip angle = 20°; 170 slices; slice thickness = 1 mm; no gap; Field of View (FoV) = 256 × 256 mm²; matrix = 256 × 256; in-plane resolution = 1 × 1 mm²; acquisition time = 9.7 min). Then, a high resolution Proton Density weighted

sequence was acquired perpendicularly to the long axis of the hippocampus (TR = 3500 ms; TE = 19 ms; flip angle = 150°; 13 slices; slice thickness = 2 mm; inter-slices gap = 2 mm; in-plane resolution = 0.375 × 0.375 mm², acquisition time = 7.6 min).

ROI-based method using high-resolution MRI data

Manual delineation of hippocampal subfields

Three hippocampal subfields were delineated: (i) subiculum; (ii) CA1; and (iii) CA2–CA3–CA4 and DG considered as a single region. These last subfields were pooled together in a same hippocampal area termed as "other" in what follows, as also performed in previous structural (Chételat et al., 2008; Csernansky et al., 2005; Sicotte et al., 2008; Wang et al., 2006) and functional studies (see Carr et al., 2010 for review), mainly because the very limited size of CA2, CA3 and CA4 with CA4 surrounded by DG challenges the accurate and reliable delineation of each individual subfield.

Tracing guidelines were based on hippocampal subfield anatomical descriptions from an atlas of the human hippocampus (Harding et al., 1998) based on the distinction of neurons on Nissl-stained sections of human brains according to the cellular criteria of Duvernoy (1998), and showing the details of the inner structure of the hippocampus along its long axis on successive slices at regular 3-mm intervals.

Delineations were performed manually by a single tracer (R.L.J.) blinded to the identity and age of subjects. Contrast was adjusted for each subject before delineation, so that the WM appears as black and the CerebroSpinal Fluid (CSF) appears as white. The tracing was done on slices perpendicular to the long axis of the hippocampus and begun on the more anterior slice where the hippocampus appeared. The fimbria was excluded from the ROI while the alveus, a thin layer of WM situated along the dorso-lateral surface of the hippocampus, was used as a landmark for delineating the border of the structure and included in our measurements because the WM/CSF contrast was much more obvious than the WM/GM contrast (see Fig. 1E for example). ROI were always traced in the following order: subiculum, CA1, and other.

The more anterior slice generally presented a small portion of the subiculum, separated from the amygdala by the alveus superiorly, the parahippocampal WM inferiorly, and CSF on the lateral border (Fig. 1A). When the hippocampus appeared as two bands of GM separated by a thin darker band (representing the *stratum lacunosum-moleculare*) as well discontinuous CSF spaces formed by the uncal sulcus (Fig. 1B), the subiculum corresponded to the inferior/ventral part and CA1 to the superior/dorsal part, both subfields being separated by horizontal lines on both medial and lateral edges of the hippocampus. On all slices posterior to this one, the medial border of the subiculum was always defined by tracing a horizontal line from the medio-dorsal extremity of the parahippocampal WM. As for the CA1 subfield, it first appeared on the dorsal part of the hippocampus head when the GM was separated in two bands as mentioned above (Fig. 1B). On the following slice, CA1 only included both lateral ends of the superior/dorsal GM band (Fig. 1C), while the middle digitation of this superior GM band corresponded to the "other" subfield. Vertical lines were traced to separate CA1 from other subfields on this slice From the next slice (Fig. 1D) and all over the body of the hippocampus (Fig. 1E to I), the CA1 ROI was constituted by the lateral part of the hippocampus including the alveus (Fig. 1D–I). Note that, in agreement with the atlas we used (Harding et al., 1998), the CA1/subiculum border was not constant along the medial–lateral axis: in the most anterior slices of the body of the hippocampus, most of the inferior part of the hippocampus was considered as subiculum (Fig. 1E) while in the most posterior slice, CA1 progressed medially (Fig. 1I). Finally the "other" ROI was traced using the alveus as a superior (inclusive) border and the vestigial hippocampal sulcus as the infero-lateral border, being careful not to include intra-hippocampal CSF spaces (as shown of Fig. 1E–F for instance).

Because of the slice thickness (2 mm) and the curvature of the hippocampus at the level of the tail, which make it very difficult to delineate the different subfields of the hippocampus, the most posterior slice where the fornix was clearly seen in full profile (Fig. 1J) was excluded from our analyses to favor the reliability of the tracings. For a minority of subjects, the following slice (that would be Fig. 1K) still included a small portion of the tail which was excluded from our analyses as well.

In average, delineations were performed on 9.05 ± 0.9 slices.

Statistical analysis

Reliability of subfield volumetric measurements was assessed by comparing volumes generated by delineating hippocampal subfields twice by the same rater in a subgroup of 15 randomly-selected subjects at a several weeks interval. The rater was blind to the identity and age of each subject. The Intraclass Correlation coefficient (ICC) was then computed.

Resultant raw volumetric measures were normalized to the Total Intracranial Volume (TIV) obtained using the VBM procedure (see below) to compensate for inter-individual variability in head size. For this step, we used the following formula : $V_{NORM} = (V_{RAW} \times TIV_{MEAN}) / TIV_{SUBJECT}$; V_{RAW} being the raw volume of the ROI for one subject, TIV_{MEAN} being the mean value of the TIV across the 50 subjects and $TIV_{SUBJECT}$ being the individual TIV value of the subject.

To assess the effect of age, education and brain hemisphere on the normalized volume of the ROI, we used a generalized linear mixed model with TIV-normalized volumes as dependant variables, age, gender, and years of education as independent variables, hemisphere as a repeated measure and first-order interactions as follow : age x gender, age × years of education, age x hemisphere. Moreover, simple correlation analyses using Pearson's *r*, were conducted on the ratios between the volume of the ROI and that of the whole brain GM (V_{ROI}/V_{GM}) on the one hand and age on the other hand, to assess the relative effect of age on hippocampal subfield volumes compared to that on global GM (a significant positive correlation between age and the ratio for a subregion would indicate that the influence of age is lower on the volume of that region than on the global GM volume).

VBM-based method

To assess the validity of a more automatic voxel-based technique classically used to assess atrophy in normal aging and pathologies compared to the reference ROI-based technique, we performed a VBM-based analysis onto the T1-weigthed MRI of the same subjects and superimposed the result map onto a 3D representation of the hippocampi, a method already used in our laboratory (Chételat et al., 2008).

Pre-processing

Pre-processing steps were performed using both the VBM5.1 and the DARTEL (Ashburner, 2007) toolboxes implemented in the Statistical Parametric Mapping software (SPM5; Wellcome department of cognitive Neurology, institute of neurology, London, England). The use of the DARTEL toolbox was motivated by the need for a precise normalization of each subject MRI and previous publications showing the benefit of using this algorithm when studying the medial temporal lobe (Yassa and Stark, 2009), leading to an increased sensitivity to detect subtle volumetric modifications within the hippocampus (Bergouignan et al., 2009).

Briefly, pre-processing consisted in: (1) Raw T1-weighted images segmentation in the native space using VBM5.1 toolbox with bias correction and the application of Hidden Markov Field weighting to enhance the quality of the segmentation; (2) importation of segmented images to DARTEL and rigid-body alignment in a common space; (3) iterative creation of specific GM templates using the DARTEL pipeline and estimation of deformation parameters ("flowfields") to warp each subject's GM segment to the final GM template; (4) spatial normalisation of raw T1 images and GM segmented data using the flowfields from the previous step; (5) modulation of resultant segments with the Jacobian determinant to account for the effects of

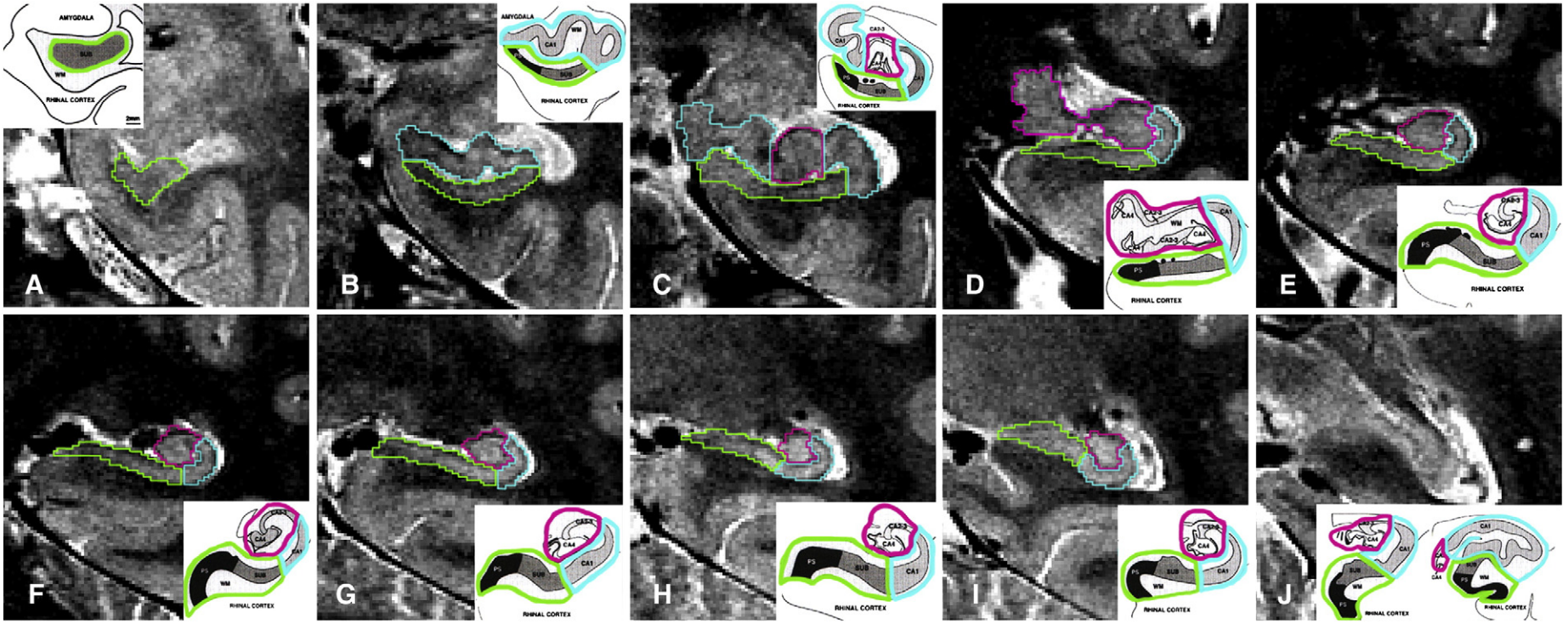

Fig. 1. Illustration of the delineation guidelines used in the present study from the description of hippocampal subfields by Harding et al. (1998), as represented on regular slices perpendicular to the grand axis of the hippocampus on the right hemisphere of an arbitrary selected subject (38-year-old male). Three Regions of Interest (ROI) were delineated: CA1 (blue), subiculum (green) and "other" (corresponding to CA2–3–4 and dentate gyrus pooled together; pink). Tracing was performed from anterior to posterior, starting on the most anterior slice where the hippocampus was visible (A) and covering the whole structure except its posterior end (J) that was excluded because the curvature of the hippocampus at that level blurred the images. For each MRI slice, the corresponding figure from Harding et al. (1998) is displayed, with the three ROI being outlined using the same color code.

local volume changes induced by the spatial normalisation and to preserve the subject's original amount of GM; and (6) smoothing of the resulting images using a 6-mm full-width at half-maximum isotropic Gaussian kernel. Note that a low smoothing kernel was intentionally used here to reduce spatial resolution degradation for the purpose of precise hippocampal assessment.

In addition to raw segmented images, we also obtained individual volumes of global GM, WM and CSF from the VBM5.1 toolbox and calculated the individual TIV by summing the volume of the three compartments. The TIV was then used for the normalisation of ROI measurements as noted above.

Statistical analyses

The effects of age were then assessed through a voxel-wise regression analysis with resultant smoothed modulated normalised GM images and introducing TIV as a nuisance variable to account for head size differences between subjects. The resultant SPM-T map was then converted to a correlation coefficient (R) map (SPM-R) using the following formulae: $R = 1/\sqrt{((n-2)/T^2+1)}$. Note that results will be presented for this simple model as the inclusion of gender and years of education as nuisance variables in the model did not change the findings.

This SPM-R map was then superimposed onto a 3D surface representation of the right and left hippocampi. These 3D representations, or hippocampal meshes, were obtained by manually delineating the hippocampi on coronal slices of the group whole brain template (obtained from the spatial normalization of raw T1 images from step 4 above). Binary ROI were then converted to 3-D meshes using the publicly available "Anatomist/BrainVISA" software (www.brainvisa.info).

In addition, to obtain an estimation of the localisation of the hippocampal subfields onto these 3D representations, the three ROI were delineated onto the DARTEL whole-brain group template following the same rules as those defined for the individual ROI described above (with however several approximations due to the lower in plane resolution) and projected onto the 3D view of both hippocampi (see Fig. 2).

Finally, to further assess the reliability of this VBM-based method to distinguish the different hippocampal subfields, simple correlations were computed between the raw volume of each ROI (CA1, subiculum and other) obtained from the ROI-based method and the smoothed modulated normalised gray matter segments, using the "multiple regression" routine in SPM. Results of this regression analysis were then superimposed onto the previously described 3D meshes of the hippocampi.

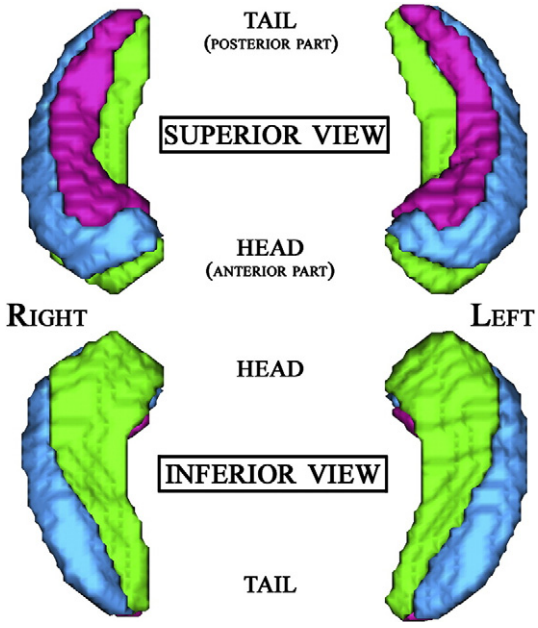

Fig. 2. Three-dimensional representation of the CA1 (blue), subiculum (green) and other (pink) subfields obtained by manual delineation of the three hippocampal subfields onto the DARTEL whole-brain group template, using landmarks adapted from Harding et al. (1998).

Table 1
Results of the generalized linear mixed model assessing the effect of age, gender, education and hemisphere onto the TIV-corrected volume of the three hippocampal subparts and that of the whole hippocampus.

	Whole hippocampus		CA1		Subiculum		Other	
	F	*p*	*F*	*p*	*F*	*p*	*F*	*p*
Age	7.90	0.007	3.52	0.07	22.79	<0.0001	0.44	0.51
Education	1.89	0.18	0.37	0.55	0.96	0.33	3.40	0.07
Gender	1.62	0.21	1.30	0.26	1.42	0.24	0.63	0.43
Hemisphere	25.71	<0.0001	7.02	0.01	11.6	0.001	2.32	0.13
Age × Education	0.22	0.64	1.00	0.32	1.47	0.23	1.67	0.20
Age × Gender	0.01	0.92	0.75	0.39	0.94	0.34	0.01	0.96
Age × Hemisphere	0.53	0.47	1.11	0.30	6.11	0.02	0.14	0.71

Results

Reliability

The intra-class correlation coefficients (ICC) were as follows: CA1 = 0.94; Subiculum = 0.89; other = 0.96.

Effect of age

ROI-based method

Results of the generalized mixed model are presented in Table 1. Concerning the whole hippocampus, main effects of hemisphere (Right>Left; $F = 22.71$, $p < 0.0001$) and age were found with lower volume being associated to increased age ($F = 7.9$, $p = 0.007$) but there were no effect of the other variables (gender, education) and no significant interaction. Regarding the hippocampal subfields, an effect of hemisphere (Right>Left) was found for both CA1 and subiculum subfields, while a significant effect of age was only found for the subiculum ($F = 22.79$, $p < 0.0001$). A significant interaction between age and hemisphere was also observed for the subiculum, indicating a stronger effect of age on the right than on the left volume ($F = 6.1$, $p = 0.02$). There was no effect of gender or education on any volumes nor any interaction between these variables and age. These findings are illustrated in Fig. 3 providing plots of ROI volume against age.

As regard to V_{ROI}/V_{GM} ratios, findings were identical on both hemispheres so that results presented here are those of bilateral volumes (sum of right and left volumes). A significant positive correlation with age was found for the whole hippocampus ($r = 0.55$; $p < 0.0001$), as well as for both CA1 ($r = 0.46$, $p = 0.0009$) and other ($r = 0.60$, $p < 0.0001$) subfields, while no correlation was found with the subiculum ($r = 0.06$, $p = 0.70$). Those findings are illustrated in Fig. 4.

VBM-based method

Fig. 5 illustrates the result of the voxel wise regression between age and GM volume projected onto a 3D view. Areas of strongest significance are located on the medial edge of both hippocampi, mainly corresponding to the subiculum subfield, whereas GM along the lateral sides (corresponding to CA1) appears to be poorly correlated to age.

Consistency between the ROI-based and the VBM-based approaches

Results of the regression analysis between the bilateral (sum of right and left) volumes of the hippocampal subfields obtained from the ROI analysis and the T1-weighted VBM-derived gray matter segments are

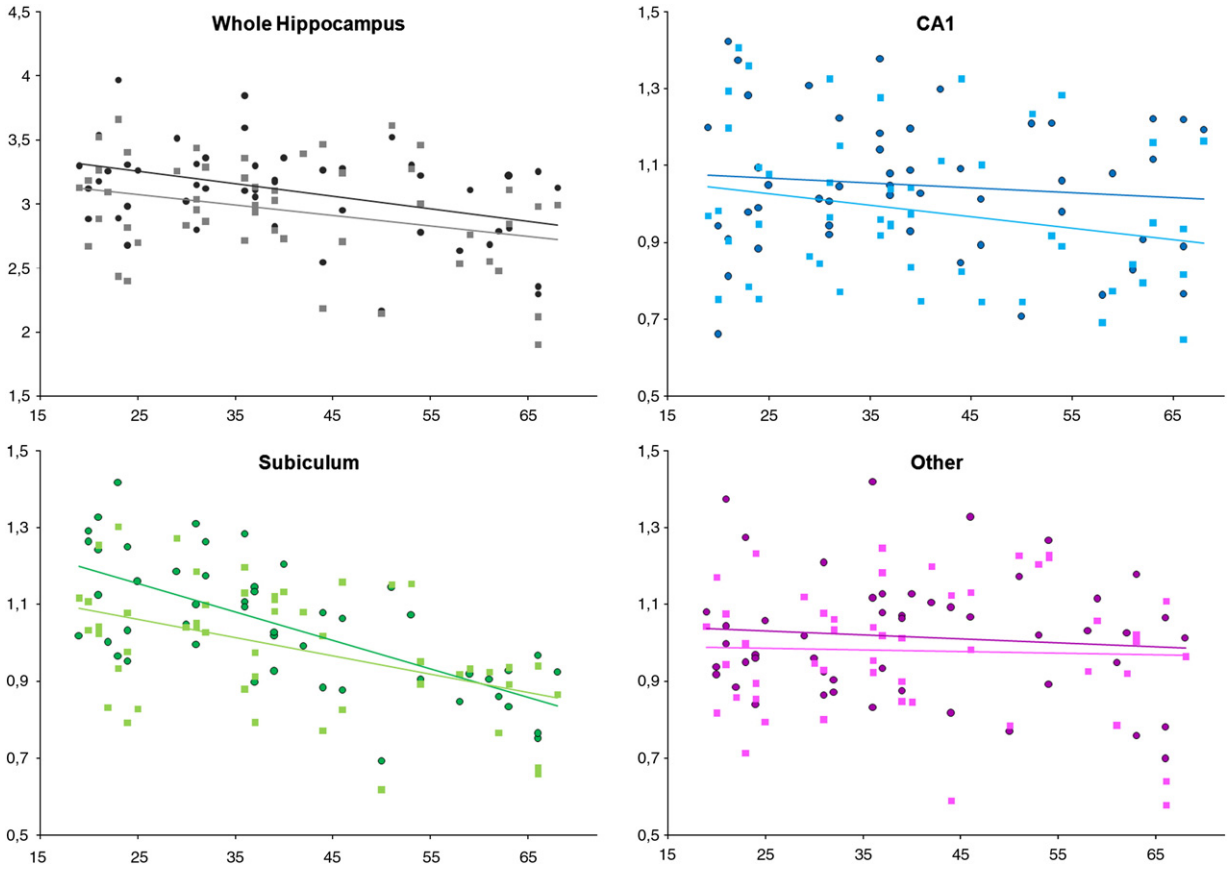

Fig. 3. Scatterplots of TIV-normalized volumes of the whole hippocampus as well as each subfield against age, for both right (dark circles) and left (light squares) hemispheres, illustrating the results from the generalized linear mixed model, i.e., a significant main effect of age on the volume of the whole hippocampus and the subiculum as well as a significant age × hemisphere interaction for the subiculum.

presented in Fig. 6. ROI-based individual CA1 volume showed a significant correlation with GM volume in the head and dorso-lateral border of the hippocampus, bilaterally. By contrast, the subiculum volume significantly correlated to GM along the medial edges of the hippocampus but showed no relationship with its lateral borders. Regarding the "other" subfield, the results were less specifically localized with areas of strongest correlation scattered in different locations including the head and the middle superior part of the body of both hippocampi.

Note that the analyses were also performed using the right and left values separately, but highly similar findings were obtained so that only the findings for the bilateral ROI are presented here.

Discussion

In the present study, we provide detailed guidelines for individual hippocampal subfield delineation using an MR-sequence especially designed for that purpose, and show a high reliability in the resulting volumetric measurements. Applying this method to a cohort of 50 healthy subjects aged 19 to 68 years old, we found a predominant effect of age on the subiculum, whose volume decreased at a same rate as global GM. By contrast, the other hippocampal subfields (Cornu Ammonis and Dentate Gyrus subfields) were found to be relatively preserved, i.e., more resistant to age than the global cerebral GM. Finally, a similar contrasted effect of age on the hippocampal subfields was obtained using a more automatic VBM-based method, which thus appeared as a reliable automatic alternative method at least to assess the CA1 versus the subiculum subfields.

Our finding of a significant effect of age on the subiculum is consistent with previous post-mortem studies (Simic et al., 1997; West et al., 1994) as well as previous neuroimaging reports (Chételat et al., 2008; Frisoni et al., 2008). In contrast to the present study however, some of these previous reports found a significant effect of age on the CA1 subfield as well (Frisoni et al., 2008; Simic et al., 1997), and the CA1 was the only subfield found to show a significant age-effect in another previous study (Mueller et al., 2007). Methodological differences between the present investigation and previous ones likely explain these discrepancies. First, the use of a surface-based approach may reveal peaks of inward deformation located in the CA1 subfield that would not result in significant differences in the volume of the whole CA1 subfield. Only Mueller et al. (Mueller et al., 2007; Mueller and Weiner, 2009) used a manual volumetric approach as employed in the present study to evaluate the effect of age. The discrepancy between our findings and theirs might arise from differences in delineation procedures. As mentioned in the Introduction section, delineations were performed on 3 consecutives 2-mm-thick slices in Mueller et al. (Mueller et al., 2007; Mueller and Weiner, 2009) so that most of the head and the tail were missing, whereas our measurements were performed on nine 2-mm-thick slices in average, evenly distributed over the whole extent of the hippocampus apart from its very posterior end. Moreover, different anatomical landmarks were used, especially for the subiculum. Thus, to improve the reliability of the measure, Mueller et al. intentionally included parts of the subiculum (prosubiculum and subiculum proper) in the CA1 ROI. It is thus possible that the effect of age on CA1 volume found in Mueller et al.'s studies reflected an age effect on these parts of the subiculum that were included in the subiculum subfield in our study. Note that the definition of the CA1-subiculum boundary is particularly inconsistent across neuroimaging studies, using either a very medial position leading to an over-estimation of the volume of CA1 (Mueller et al., 2007; Yushkevich et al., 2009) or the lateral extremity resulting in over-estimating the subiculum volume (Hayman et al., 1998; Van Leemput et al., 2009). This difference may explain general discrepancies between studies regarding the

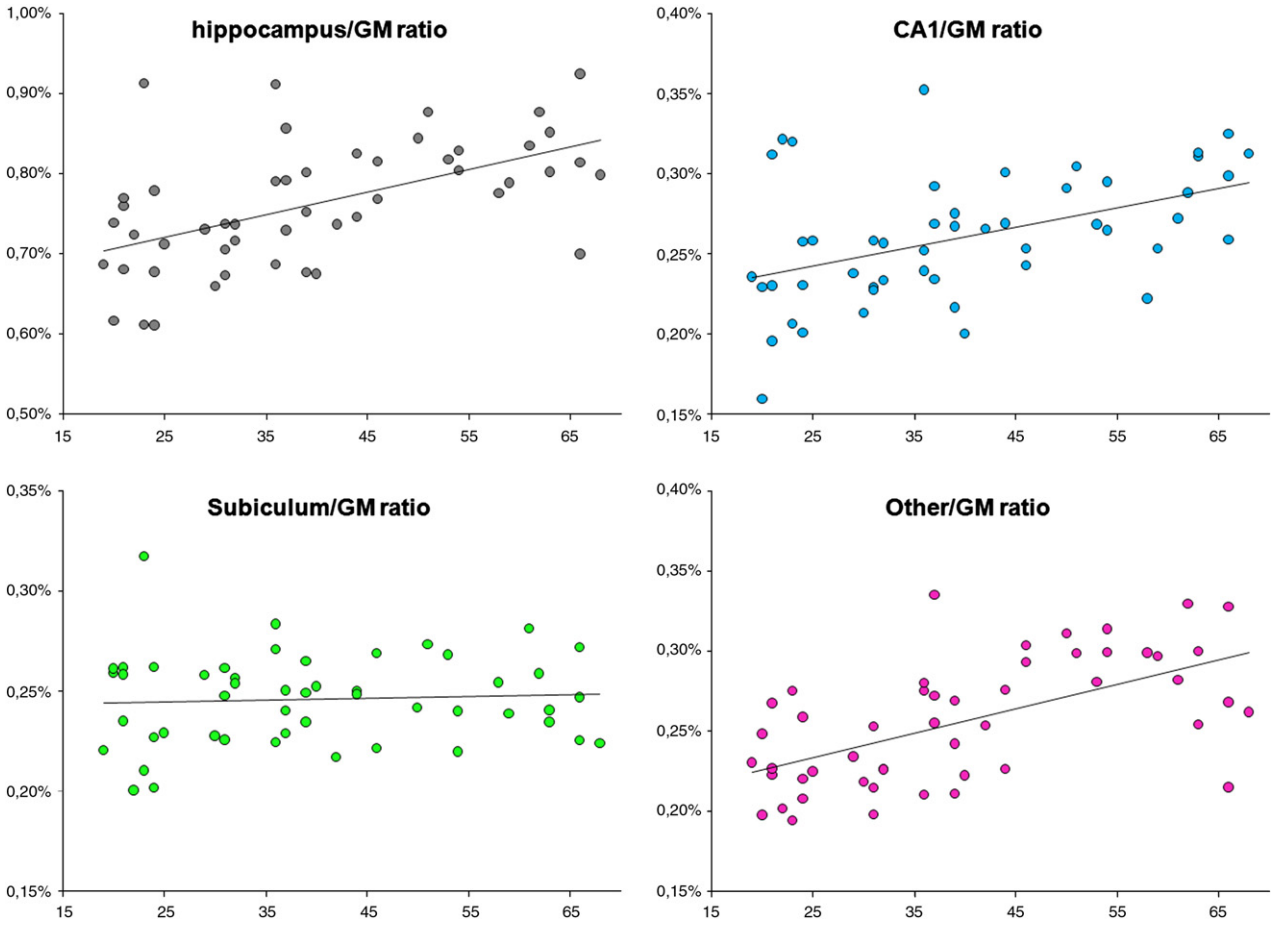

Fig. 4. Scatterplots of the correlations between age and the ratio between the volume of each ROI (right and left pooled) and that of the whole-brain GM. A significant positive correlation with age was observed for all ratios except for the subiculum/GM ratio.

assessment of the volume of those two subfields. Lastly, discrepancies may also be due to differences in the ages of the samples; the age range covered in the present study (19 to 68 years) does not include the oldest edge by contrast to that of Mueller et al. (22 to 85 years) and Frisoni et al. (66 to 82 years). As some previous findings suggest that decrease in the volume of the whole hippocampus is more pronounced at an advanced age (Allen et al., 2005; Fjell et al., 2009; Raz et al., 2004), especially for CA1 whose atrophy has been reported for subjects above 60 years (Mueller et al., 2007), the lack of a significant effect of age on CA1 in the present study might be related to the lack of subjects in the seventh decade. Note that we also used a quadratic approach to test for the hypothesis of a non-linear effect of age on the volume of the hippocampal subfields (and more specifically an increase shrinkage in the last decades), but we failed to evidence any significant non-linear effect (see supplementary materials). These negative findings are likely due to the fact that our sample size was not large enough to detect non-linear effects, or to the lack of subjects above 70 years, as the three studies mentioned above that reported an increasing rate of atrophy with age all included subjects over 70.

Yet, it is also possible that CA1 atrophy in the oldest reflects pathological, instead of normal aging, processes, as older populations are more likely to include cases at a presymptomatic stage of AD that may drive the correlation (Fjell et al., 2009). Only longitudinal studies performing a clinical follow-up of the subjects over years to ensure they do not progress to dementia would allow controlling for this potential bias. Raji et al. (2009) recently performed a VBM analysis on 169 healthy controls over 70 years old who remained cognitively normal over 5 years following the MRI acquisition. Interestingly, their results were very similar to ours, with a strongest effect of age on the medial border of both hippocampi while the lateral sides (i.e., CA1) were spared, comforting the idea that CA1 atrophy might reflect pre-symptomatic AD-related processes instead of normal aging.

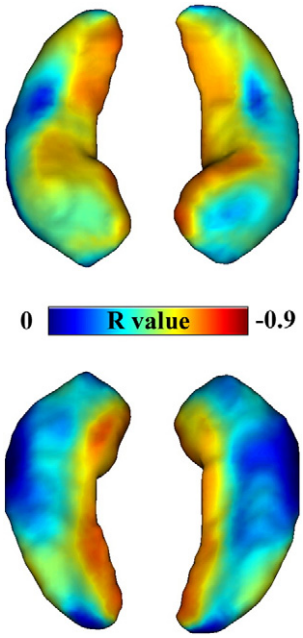

Fig. 5. Result of the voxel-based regression between age and GM across the whole sample ($n = 50$). The SPM-R map was superimposed onto a 3D view of the hippocampi. Warm colors (red) indicate a strong negative correlation between age and GM volume.

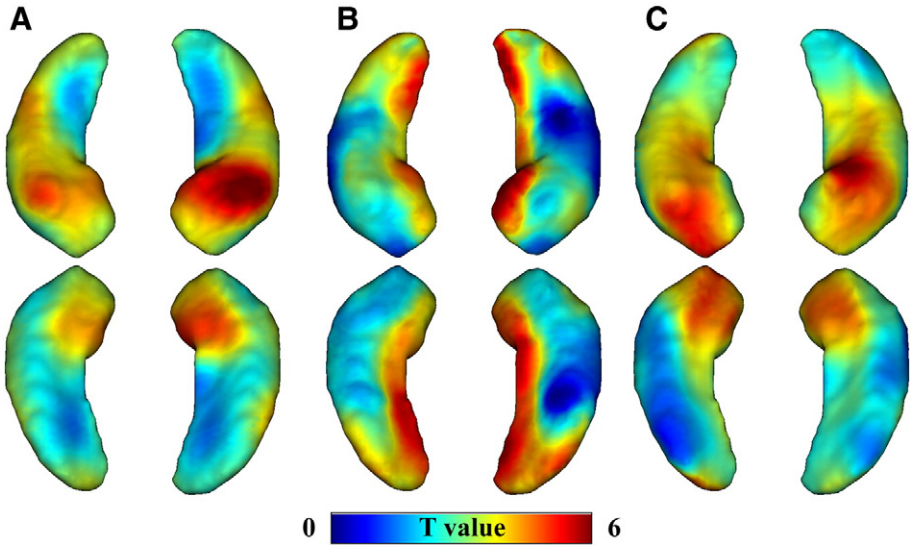

Fig. 6. Results of the voxel-based regression between the T1-weighted gray matter segments and (A) CA1 volume; (B) subiculum volume; (C) other volume. Bilateral (right + left) volumes obtained thanks to manual tracing of individual subfields were used in these analyses.

While the mechanisms underlying the differential vulnerability of hippocampal regions are unknown, it is worth noting that the subfields found to resist to age, i.e. the gyrus dentatus and CA subfields, all consist in three-layered archicortex, while both the global cerebral GM and the subiculum found to shrink with age are made of more recently evolved cortex, i.e. the neocortex and the mesocortex (which is a transitional area between archicortex and neocortex), respectively. These observations support the "developmental hypothesis" (Davis et al., 2009; Grieve et al., 2005; Kalpouzos et al., 2009; Kennedy and Raz, 2009) according to which the first cerebral structures to develop, phylogenetically as well as ontogenetically, are the most resistant to the effects of age and vice-versa ("first-in last-out" theory).

Interestingly, the preservation of the CA1 subfield evidenced here contrasts with the pattern of atrophy described in AD. Indeed, this particular subfield is constantly reported as the more vulnerable in post-mortem (Price et al., 2001; West et al., 1994) as well as in neuroimaging (Apostolova et al., 2008; Chételat et al., 2008; Csernansky et al., 2005; Frisoni et al., 2008; Mueller and Weiner, 2009; Wang et al., 2003, 2006) studies. This suggests that CA1 could be particularly helpful to early AD detection, and especially to distinguish the effect of the pathology from that of normal aging. It may even be more accurate than the volume of the whole hippocampus for early diagnosis, as the latter was found to decline with age in the present study consistently with some, though not all, previous reports (see Introduction). This may explain the suboptimal diagnosis accuracy of hippocampal atrophy when considering the structure as a whole despite its early and marked structural alteration over the course of the disease (Chételat and Baron, 2003; Frisoni et al., 2010; Ramani et al., 2006). Future studies in MCI and AD comparing the diagnostic accuracy of hippocampal subfields to that of the whole hippocampus would allow to confirm this hypothesis.

The present study has several limitations. First, a longitudinal approach would be more appropriate than a cross-sectional study to assess the effect of age as it is not biased by potential cohort effects. Second, our sample size is quite limited considering the age range (19 to 68 years) and especially to assess non-linear effects (see above). Finally, we decided to sample the hippocampus over most of his long axis. However, because of acquisition time constraints, we then had to use a 2-mm gap between slices. Also, to improve the reproducibility and accuracy of measurements, we decided to exclude the most posterior slice(s). As a result, the acquisition did not cover the whole hippocampus and more precise measurements could be obtained if we could obtain acquisitions of the entire structure without increasing the acquisition time.

As a whole, the present study provides a reliable method to delineate hippocampal subfields using a specific clinically relevant MR sequence, and validates an alternative automatic voxel-based approach. Both methods consistently pointed to a predominant effect of age on the subiculum while other hippocampal subfields, including the CA1 known to be particularly vulnerable to AD, were relatively preserved. This technique may prove to be particularly useful not only for early AD diagnosis, but also for application to other disorders characterized by hippocampal atrophy.

Acknowledgments

The authors acknowledge the financial support from the ANR (Agence Nationale de la Recherche. Longévité et Vieillissement, 2007), the Inserm and Region Basse-Normandie for this project. They are grateful to F. Lamberton and N. Delcroix for their help in the development of the MR sequence as well as M. Camus, V. de la Sayette, C. Schupp, J. Dayan, M. Groussard, C. Lebouleux, M.H. Noel & M.C. Onfroy for their participation in data acquisition. Finally, they would like to thank P. Maillard and J. Gonneaud for their precious help in the statistical analyses.

Appendix A. Supplementary data

Supplementary data associated with this article can be found, in the online version, at doi:10.1016/j.neuroimage.2010.06.024.

References

Allen, J.S., Bruss, J., Brown, C.K., Damasio, H., 2005. Normal neuroanatomical variation due to age: the major lobes and a parcellation of the temporal region. Neurobiol. Aging 26, 1245–1260.

Apostolova, L.G., Dutton, R.A., Dinov, I.D., Hayashi, K.M., Toga, A.W., Cummings, J.L., Thompson, P.M., 2006. Conversion of mild cognitive impairment to Alzheimer disease predicted by hippocampal atrophy maps. Arch. Neurol. 63, 693–699.

Apostolova, L.G., Mosconi, L., Thompson, P.M., Green, A.E., Hwang, K.S., Ramirez, A., Mistur, R., Tsui, W.H., de Leon, M.J., 2008. Subregional hippocampal atrophy predicts Alzheimer's dementia in the cognitively normal. Neurobiol. Aging.

Ashburner, J., 2007. A fast diffeomorphic image registration algorithm. Neuroimage 38, 95–113.

Barboriak, D.P., Doraiswamy, P.M., Krishnan, K.R., Vidyarthi, S., Sylvester, J., Charles, H.C., 2000. Hippocampal sulcal cavities on MRI: relationship to age and apolipoprotein E genotype. Neurology 54, 2150–2153.

Bastos-Leite, A.J., van Waesberghe, J.H., Oen, A.L., van der Flier, W.M., Scheltens, P., Barkhof, F., 2006. Hippocampal sulcus width and cavities: comparison between patients with Alzheimer disease and nondemented elderly subjects. AJNR Am. J. Neuroradiol. 27, 2141–2145.

Bergouignan, L., Chupin, M., Czechowska, Y., Kinkingnehun, S., Lemogne, C., Le, B.G., Lepage, M., Garnero, L., Colliot, O., Fossati, P., 2009. Can voxel based morphometry, manual segmentation and automated segmentation equally detect hippocampal volume differences in acute depression? Neuroimage 45, 29–37.
Bird, C.M., Burgess, N., 2008. The hippocampus and memory: insights from spatial processing. Nat. Rev. Neurosci. 9, 182–194.
Burgess, N., Maguire, E.A., O'Keefe, J., 2002. The human hippocampus and spatial and episodic memory. Neuron 35, 625–641.
Carr, V.A., Rissman, J., Wagner, A.D., 2010. Imaging the human medial temporal lobe with high-resolution fMRI. Neuron 65, 298–308.
Chételat, G., Baron, J.C., 2003. Early diagnosis of Alzheimer's disease: contribution of structural neuroimaging. Neuroimage 18, 525–541.
Chételat, G., Fouquet, M., Kalpouzos, G., Denghien, I., de la Sayette, V., Viader, F., Mézenge, F., Landeau, B., Baron, J.C., Eustache, F., Desgranges, B., 2008. Three-dimensional surface mapping of hippocampal atrophy progression from MCI to AD and over normal aging as assessed using voxel-based morphometry. Neuropsychologia 46, 1721–1731.
Cho, Z.H., Han, J.Y., Hwang, S.I., Kim, D.S., Kim, K.N., Kim, N.B., Kim, S.J., Chi, J.G., Park, C.W., Kim, Y.B., 2010. Quantitative analysis of the hippocampus using images obtained from 7.0 T MRI. Neuroimage 49, 2134–2140.
Csernansky, J.G., Wang, L., Swank, J., Miller, J.P., Gado, M., McKeel, D., Miller, M.I., Morris, J.C., 2005. Preclinical detection of Alzheimer's disease: hippocampal shape and volume predict dementia onset in the elderly. Neuroimage 25, 783–792.
Davis, S.W., Dennis, N.A., Buchler, N.G., White, L.E., Madden, D.J., Cabeza, R., 2009. Assessing the effects of age on long white matter tracts using diffusion tensor tractography. Neuroimage 46, 530–541.
De Vita, E., Thomas, D.L., Roberts, S., Parkes, H.G., Turner, R., Kinchesh, P., Shmueli, K., Yousry, T.A., Ordidge, R.J., 2003. High resolution MRI of the brain at 4.7 Tesla using fast spin echo imaging. Br. J. Radiol. 76, 631–637.
Duvernoy, H.M., 1998. The human hippocampus, functional anatomy, vascularization, and serial sections with MRI, 2nd ed. Springer, Berlin.
Ekstrom, A.D., Kahana, M.J., Caplan, J.B., Fields, T.A., Isham, E.A., Newman, E.L., Fried, I., 2003. Cellular networks underlying human spatial navigation. Nature 425, 184–188.
Eldridge, L.L., Engel, S.A., Zeineh, M.M., Bookheimer, S.Y., Knowlton, B.J., 2005. A dissociation of encoding and retrieval processes in the human hippocampus. J. Neurosci. 25, 3280–3286.
Eriksson, S.H., Thom, M., Bartlett, P.A., Symms, M.R., McEvoy, A.W., Sisodiya, S.M., Duncan, J.S., 2008. PROPELLER MRI visualizes detailed pathology of hippocampal sclerosis. Epilepsia 49, 33–39.
Fjell, A.M., Walhovd, K.B., Fennema-Notestine, C., McEvoy, L.K., Hagler, D.J., Holland, D., Brewer, J.B., Dale, A.M., 2009. One-year brain atrophy evident in healthy aging. J. Neurosci. 29, 15223–15231.
Frisoni, G.B., Ganzola, R., Canu, E., Rub, U., Pizzini, F.B., Alessandrini, F., Zoccatelli, G., Beltramello, A., Caltagirone, C., Thompson, P.M., 2008. Mapping local hippocampal changes in Alzheimer's disease and normal ageing with MRI at 3 Tesla. Brain 131, 3266–3276.
Frisoni, G.B., Fox, N.C., Jack Jr., C.R., Scheltens, P., Thompson, P.M., 2010. The clinical use of structural MRI in Alzheimer disease. Nat. Rev. Neurol. 6, 67–77.
Geuze, E., Vermetten, E., Bremner, J.D., 2005. MR-based in vivo hippocampal volumetrics: 2. Findings in neuropsychiatric disorders. Mol. Psychiatry 10, 160–184.
Good, C.D., Johnsrude, I.S., Ashburner, J., Henson, R.N., Friston, K.J., Frackowiak, R.S., 2001. A voxel-based morphometric study of ageing in 465 normal adult human brains. Neuroimage 14, 21–36.
Grieve, S.M., Clark, C.R., Williams, L.M., Peduto, A.J., Gordon, E., 2005. Preservation of limbic and paralimbic structures in aging. Hum. Brain Mapp. 25, 391–401.
Harding, A.J., Halliday, G.M., Kril, J.J., 1998. Variation in hippocampal neuron number with age and brain volume. Cereb. Cortex 8, 710–718.
Hayman, L.A., Fuller, G.N., Cavazos, J.E., Pfleger, M.J., Meyers, C.A., Jackson, E.F., 1998. The hippocampus: normal anatomy and pathology. AJR Am. J. Roentgenol. 171, 1139–1146.
Jack Jr, C.R., Petersen, R.C., O'Brien, P.C., Tangalos, E.G., 1992. MR-based hippocampal volumetry in the diagnosis of Alzheimer's disease. Neurology 42, 183–188.
Jack Jr., C.R., Petersen, R.C., Xu, Y.C., Waring, S.C., O'Brien, P.C., Tangalos, E.G., Smith, G.E., Ivnik, R.J., Kokmen, E., 1997. Medial temporal atrophy on MRI in normal aging and very mild Alzheimer's disease. Neurology 49, 786–794.
Kalpouzos, G., Chételat, G., Baron, J.C., Landeau, B., Mevel, K., Godeau, C., Barré, L., Constans, J.M., Viader, F., Eustache, F., Desgranges, B., 2009. Voxel-based mapping of brain gray matter volume and glucose metabolism profiles in normal aging. Neurobiol. Aging 30, 112–124.
Kennedy, K.M., Raz, N., 2009. Pattern of normal age-related regional differences in white matter microstructure is modified by vascular risk. Brain Res. 1297, 41–56.
Lemaitre, H., Crivello, F., Grassiot, B., Alperovitch, A., Tzourio, C., Mazoyer, B., 2005. Age- and sex-related effects on the neuroanatomy of healthy elderly. Neuroimage 26, 900–911.
Lepage, M., Habib, R., Tulving, E., 1998. Hippocampal PET activations of memory encoding and retrieval: the HIPER model. Hippocampus 8, 313–322.
Li, Y., Li, J., Segal, S., Wegiel, J., De, S.S., Zhan, J., de Leon, M.J., 2006. Hippocampal cerebrospinal fluid spaces on MR imaging: relationship to aging and Alzheimer disease. AJNR Am. J. Neuroradiol. 27, 912–918.
Maguire, E.A., Burgess, N., Donnett, J.G., Frackowiak, R.S., Frith, C.D., O'Keefe, J., 1998. Knowing where and getting there: a human navigation network. Science 280, 921–924.
Malykhin, N.V., Bouchard, T.P., Camicioli, R., Coupland, N.J., 2008. Aging hippocampus and amygdala. NeuroReport 19, 543–547.
Malykhin, N.V., Lebel, R.M., Coupland, N.J., Wilman, A.H., Carter, R., 2010. In vivo quantification of hippocampal subfields using 4.7 T fast spin echo imaging. Neuroimage 49, 1224–1230.
Mattis, S., 1976. Mental status examination for organic mental syndrome in the elderly patient. In: Bellack, L., Karasu, T.B. (Eds.), Mental status examination for organic mental syndrome in the elderly patients. Grune & Stratton, New York, pp. 77–101.
Mueller, S.G., Weiner, M.W., 2009. Selective effect of age, Apo e4, and Alzheimer's disease on hippocampal subfields. Hippocampus 19, 558–564.
Mueller, S.G., Stables, L., Du, A.T., Schuff, N., Truran, D., Cashdollar, N., Weiner, M.W., 2007. Measurement of hippocampal subfields and age-related changes with high resolution MRI at 4T. Neurobiol. Aging 28, 719–726.
Mueller, S.G., Schuff, N., Raptentsetsang, S., Elman, J., Weiner, M.W., 2008. Selective effect of Apo e4 on CA3 and dentate in normal aging and Alzheimer's disease using high resolution MRI at 4 T. Neuroimage 42, 42–48.
Nakada, T., Kwee, I.L., Fujii, Y., Knight, R.T., 2005. High-field, T2 reversed MRI of the hippocampus in transient global amnesia. Neurology 64, 1170–1174.
Pan, J.W., Vaughan, J.T., Kuzniecky, R.I., Pohost, G.M., Hetherington, H.P., 1995. High resolution neuroimaging at 4.1T. Magn. Reson. Imaging 13, 915–921.
Price, J.L., Ko, A.I., Wade, M.J., Tsou, S.K., McKeel, D.W., Morris, J.C., 2001. Neuron number in the entorhinal cortex and CA1 in preclinical Alzheimer disease. Arch. Neurol. 58, 1395–1402.
Raji, C.A., Lopez, O.L., Kuller, L.H., Carmichael, O.T., Becker, J.T., 2009. Age, Alzheimer disease, and brain structure. Neurology 73, 1899–1905.
Ramani, A., Jensen, J.H., Helpern, J.A., 2006. Quantitative MR imaging in Alzheimer disease. Radiology 241, 26–44.
Raz, N., Rodrigue, K.M., Head, D., Kennedy, K.M., Acker, J.D., 2004. Differential aging of the medial temporal lobe: a study of a five-year change. Neurology 62, 433–438.
Seab, J.P., Jagust, W.J., Wong, S.T., Roos, M.S., Reed, B.R., Budinger, T.F., 1988. Quantitative NMR measurements of hippocampal atrophy in Alzheimer's disease. Magn. Reson. Med. 8, 200–208.
Sicotte, N.L., Kern, K.C., Giesser, B.S., Arshanapalli, A., Schultz, A., Montag, M., Wang, H., Bookheimer, S.Y., 2008. Regional hippocampal atrophy in multiple sclerosis. Brain 131, 1134–1141.
Simic, G., Kostovic, I., Winblad, B., Bogdanovic, N., 1997. Volume and number of neurons of the human hippocampal formation in normal aging and Alzheimer's disease. J. Comp. Neurol. 379, 482–494.
Spaniol, J., Davidson, P.S., Kim, A.S., Han, H., Moscovitch, M., Grady, C.L., 2009. Event-related fMRI studies of episodic encoding and retrieval: meta-analyses using activation likelihood estimation. Neuropsychologia 47, 1765–1779.
Squire, L.R., Ojemann, J.G., Miezin, F.M., Petersen, S.E., Videen, T.O., Raichle, M.E., 1992. Activation of the hippocampus in normal humans: a functional anatomical study of memory. Proc. Natl Acad. Sci. USA 89, 1837–1841.
Sullivan, E.V., Marsh, L., Pfefferbaum, A., 2005. Preservation of hippocampal volume throughout adulthood in healthy men and women. Neurobiol. Aging 26, 1093–1098.
Suthana, N.A., Ekstrom, A.D., Moshirvaziri, S., Knowlton, B., Bookheimer, S.Y., 2009. Human hippocampal CA1 involvement during allocentric encoding of spatial information. J. Neurosci. 29, 10512–10519.
Theysohn, J.M., Kraff, O., Maderwald, S., Schlamann, M.U., de, G.A., Forsting, M., Ladd, S.C., Ladd, M.E., Gizewski, E.R., 2009. The human hippocampus at 7 T—in vivo MRI. Hippocampus 19, 1–7.
Thomas, B.P., Welch, E.B., Niederhauser, B.D., Whetsell Jr., W.O., Anderson, A.W., Gore, J.C., Avison, M.J., Creasy, J.L., 2008. High-resolution 7T MRI of the human hippocampus in vivo. J. Magn. Reson. Imaging 28, 1266–1272.
Thompson, P.M., Hayashi, K.M., De Zubicaray, G.I., Janke, A.L., Rose, S.E., Semple, J., Hong, M.S., Herman, D.H., Gravano, D., Doddrell, D.M., Toga, A.W., 2004. Mapping hippocampal and ventricular change in Alzheimer disease. Neuroimage 22, 1754–1766.
Tulving, E., Markowitsch, H.J., 1998. Episodic and declarative memory: role of the hippocampus. Hippocampus 8, 198–204.
Van Leemput, K., Bakkour, A., Benner, T., Wiggins, G., Wald, L.L., Augustinack, J., Dickerson, B.C., Golland, P., Fischl, B., 2009. Automated segmentation of hippocampal subfields from ultra-high resolution in vivo MRI. Hippocampus 19, 549–557.
Wang, L., Swank, J.S., Glick, I.E., Gado, M.H., Miller, M.I., Morris, J.C., Csernansky, J.G., 2003. Changes in hippocampal volume and shape across time distinguish dementia of the Alzheimer type from healthy aging. Neuroimage 20, 667–682.
Wang, L., Miller, J.P., Gado, M.H., McKeel, D.W., Rothermich, M., Miller, M.I., Morris, J.C., Csernansky, J.G., 2006. Abnormalities of hippocampal surface structure in very mild dementia of the Alzheimer type. Neuroimage 30, 52–60.
West, M.J., Coleman, P.D., Flood, D.G., Troncoso, J.C., 1994. Differences in the pattern of hippocampal neuronal loss in normal ageing and Alzheimer's disease. Lancet 344, 769–772.
Yassa, M.A., Stark, C.E., 2009. A quantitative evaluation of cross-participant registration techniques for MRI studies of the medial temporal lobe. Neuroimage 44, 319–327.
Yoneoka, Y., Kwee, I.L., Fujii, Y., Nakada, T., 2002. Criteria for normalcy of cavities observed within the adult hippocampus: high-resolution magnetic resonance imaging study on a 3.0-T system. J. Neuroimaging 12, 231–235.
Yushkevich, P.A., Avants, B.B., Pluta, J., Das, S., Minkoff, D., Mechanic-Hamilton, D., Glynn, S., Pickup, S., Liu, W., Gee, J.C., Grossman, M., Detre, J.A., 2009. A high-resolution computational atlas of the human hippocampus from postmortem magnetic resonance imaging at 9.4 T. Neuroimage 44, 385–398.
Zeineh, M.M., Engel, S.A., Thompson, P.M., Bookheimer, S.Y., 2003. Dynamics of the hippocampus during encoding and retrieval of face-name pairs. Science 299, 577–580.